Acta Pharmaceutica Sinica B 2020;10(5):895–902

Chinese Pharmaceutical Association
Institute of Materia Medica, Chinese Academy of Medical Sciences

Acta Pharmaceutica Sinica B

www.elsevier.com/locate/apsb
www.sciencedirect.com

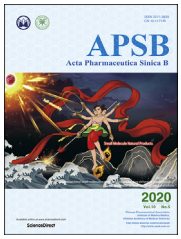

ORIGINAL ARTICLE

Indole alkaloid glycosides with a 1′-(phenyl)ethyl unit from *Isatis indigotica* leaves

Qinglan Guo, Dawei Li, Chengbo Xu, Chenggen Zhu, Ying Guo, Haibo Yu, Xiaoliang Wang, Jiangong Shi*

State Key Laboratory of Bioactive Substance and Function of Natural Medicines, Institute of Materia Medica, Chinese Academy of Medical Sciences and Peking Union Medical College, Beijing 100050, China

Received 6 July 2019; received in revised form 27 August 2019; accepted 3 September 2019

KEY WORDS

Cruciferae;
Isatis indigotica;
Indole alkaloid glycoside;
Isatidifoliumosides;
Epiisatidifoliumosides;
KCNQ2 inhibition;
Anti-influenza;
Anti-virus;
Activity

Abstract Seven indole alkaloid glycosides containing a 1′-(4″-hydroxy-3″,5″-dimethoxyphenyl)ethyl unit (**1**–**7**) were isolated from an aqueous extract of *Isatis indigotica* leaves (da qing ye). Their structures were determined by spectroscopic data analysis combined with enzymatic hydrolysis as well as comparison of their experimental CD (circular dichroism) and calculated ECD (electrostatic circular dichroism) spectra. Based on analysis of $[\alpha]_D^{20}$ and/or Cotton effect (CE) data of **1**–**7**, two simple roles to assign location and/or configuration of β-glycopyranosyloxy and 1′-(phenyl)ethyl units in the indole alkaloid glycosides are proposed. Stereoselectivity in plausible biosynthetic pathways of **1**–**7** is discussed. Compounds **3** and **4** and their mixture in a 3:2 ratio showed activity against KCNQ2 in CHO cells. The mixture of **5** and **6** (3:2) exhibited antiviral activity against influenza virus H1N1 PR8 with IC_{50} 64.7 μmol/L (ribavirin, IC_{50} 54.3 μmol/L), however, the individual **5** or **6** was inactive. Preliminary structure–activity relationships were observed.

1. Introduction

Isatis indigotica Fort. (Cruciferae) is a widely cultivated medicinal plant. The dried leaves and roots of this plant, named “da qing ye” and “ban lan gen” in Chinese, respectively, are used in traditional Chinese medicines for the treatment of influenza and other infections[1]. Diverse bioactive constituents have been reported from ethanol or methanol extracts of the *I. indigotica* leaves and roots[2–25]. However, few works were done on the chemical constituents of decoctions of the two herbal medicines[7,13,14,16,18,24] though the

*Corresponding author. Tel.: +86 10 63025166; fax: +86 10 63017757.
E-mail address: shijg@imm.ac.cn (Jiangong Shi).

Peer review under responsibility of Institute of Materia Medica, Chinese Academy of Medical Sciences and Chinese Pharmaceutical Association.

https://doi.org/10.1016/j.apsb.2019.09.001

decoctions are practically applied in traditional Chinese medicine. Therefore, the aqueous extracts of "ban lan gen" and "da qing ye" were successively investigated as part of our program to systematically assess the chemical diversity and pharmacological activity of traditional Chinese medicines focusing on the minor components[26–39]. From the "ban lan gen" extract, 57 new alkaloids including 22 indole and bisindole alkaloid glycosides were isolated, and some of them showed antiviral activity[40–55]. Previously we reported two pairs of unusual scalemic enantiomers isatidifoliumindolinones A−D from the "da qing ye" extract[56], this paper deals with isolation, structural elucidation, biosynthetic postulation, and biological activity of seven unusual indole alkaloid glycosides (**1**−**7**), including three pairs of epimers named isatidifoliumosides/epiisatidifoliumosides A (**1/2**), B (**3/4**), and C (**5/6**), respectively, and an isomer named isatidifoliumoside D (**7**) (Fig. 1). The new isolates contain a 1′-(4″-hydroxy-3″,5″-dimethoxyphenyl)ethyl moiety at different positions (N-1, C-2, or C-3) of the indole nucleus, biogenetically associating to isatidifoliumindolinones A−D[56]. Analysis of specific rotations $[\alpha]_D$ and Cotton effects (CEs) of **1**−**7** resulted in preliminary roles for assignment of location and configuration of the *β*-glycopyranosyloxy and 1′-(phenyl)ethyl units in this group of indole alkaloids. Especially, **5** and **6** are the first indole alkaloid *β*-D-allopyranosides from nature, while the mixture of **5** and **6** (3:2) showed antiviral activity against influenza virus H1N1 PR8, which represents the first bioactive indole glycosides supporting clinic application of the herbal medicine.

2. Results and discussion

Compound **1** was isolated as a white amorphous powder with $[\alpha]_D^{20}$ −23.7 (*c* 0.1, MeOH). The IR spectrum of **1** exhibited absorption bands assignable to hydroxy (3303 cm^{-1}) and aromatic ring (1613, 1519, and 1460 cm^{-1}) functional groups. Its molecular formula of $C_{24}H_{29}NO_9$ was determined by HR-ESI-MS combined with the NMR spectroscopic data (Tables 1 and 2). The NMR spectrum of **1** in CD_3OD showed resonances attributable to two *ortho*-disubstituted benzene rings at δ_H 7.69 (brd, J = 7.8 Hz, H-4), 6.97 (dt, J = 7.8, 1.2 Hz, H-5), 7.06 (ddd, J = 8.4, 7.8, 1.2 Hz, H-6), and 7.25 (brd, J = 8.4 Hz, H-7); a 1′,1′-disubstituted ethyl unit at δ_H 5.60 (q, J = 7.2 Hz, H-1′) and 1.84 (d, J = 7.2 Hz, H_3-2′); a 4″-hydroxy-3″,5″-dimethoxyphenyl at δ_H 3.73 (s, OCH_3-3″,5″) and 6.46 (s, H-2″/6″); and a trisubstituted double bond at δ_H 7.31 (s, H-2). It also displayed diagnostic resonances for a *β*-glucopyranosyl moiety (Table 1). The ^{13}C NMR and DEPT spectra showed carbon resonances corresponding

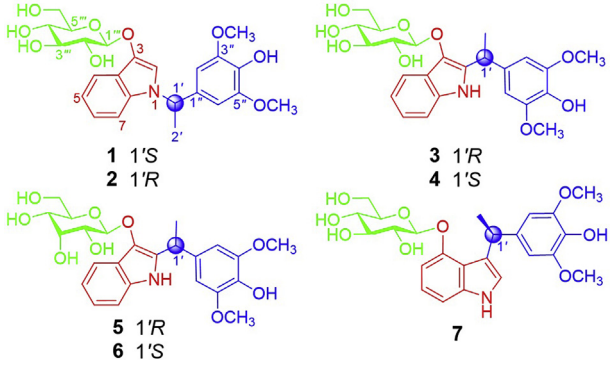

Figure 1 The structures of compounds **1**−**7**.

Table 1 ^1H NMR spectroscopic data for compounds **1**−**7** in CD_3OD[a].

No.	1	2	3	4	5	6	7
2	7.31 s	7.31 s					6.99 s
4	7.69 brd (7.8)	7.69 brd (7.8)	7.70 brd (7.8)	7.74 brd (7.8)	7.72 brd (7.8)	7.76 brd (7.8)	
5	6.97 dt (7.8, 1.2)	6.97 dt (7.8, 1.2)	6.94 dt (7.8, 1.2)	6.94 dt (7.8, 1.2)	6.94 dt (7.8, 1.2)	6.95 dt (7.8, 1.2)	6.62 brd (7.2)
6	7.06 ddd (8.4, 7.8, 1.2)	7.07 ddd (8.4, 7.8, 1.2)	7.00 dt (7.8, 1.2)	7.00 ddd (8.4, 7.8, 1.2)	7.00 dt (7.8, 1.2)	7.00 dt (7.8, 1.2)	6.94 t (7.2)
7	7.25 brd (8.4)	7.25 brd (8.4)	7.22 brd (7.8)	7.21 brd (8.4)	7.21 d (7.8)	7.21 brd (7.8)	6.97 dd (7.2, 1.2)
1′	5.60 q (7.2)	5.61 q (7.2)	4.74 q (7.2)	4.73 q (7.2)	4.74 q (7.2)	4.74 q (7.8)	4.87 q (7.2)
2′	1.84 d (7.2)	1.84 d (7.2)	1.68 d (7.2)	1.65 d (7.2)	1.67 d (7.2)	1.66 d (7.8)	1.59 d (7.2)
2″	6.46 s	6.45s	6.71 s	6.64 s	6.68 s	6.64 s	6.56 s
6″	6.46 s	6.45 s	6.71 s	6.64 s	6.68 s	6.64 s	6.56 s
1‴	4.72 d (7.2)	4.71 d (7.8)	4.62 d (8.4)	4.66 d (7.8)	5.05 d (7.8)	5.04 d (8.4)	5.06 d (7.8)
2‴	3.50 dd (9.0, 7.2)	3.50 dd (7.8, 9.0)	3.53 dd (9.0, 8.4)	3.50 dd (9.0, 7.8)	3.65 dd (7.8,3.0)	3.63 dd (8.4,3.0)	3.58 dd (9.0, 7.8)
3‴	3.44 t (9.0)	3.43 t (9.0)	3.40 t (9.0)	3.41 t (9.0)	4.17 t (3.0)	4.15 t (3.0)	3.46 t (9.0)
4‴	3.39 t (9.0)	3.38 t (9.0)	3.47 t (9.0)	3.46 t (9.0)	3.67 dd (9.6,3.0)	3.66 dd (9.6,3.0)	3.28 t (9.0)
5‴	3.36 m	3.35 m	3.14 m	3.16 m	3.62 m	3.61 m	3.41 m
6‴a	3.89 dd (12.0, 2.4)	3.89 dd (12.0, 2.4)	3.82 dd (11.4, 1.8)	3.66 m	3.83 dd (11.4, 2.4)	3.67 m	3.83 dd (12.0, 2.4)
6‴b	3.70 dd (12.0, 5.4)	3.70 dd (12.0, 5.4)	3.73 dd (11.4, 4.8)	3.66 m	3.74 dd (11.4, 4.8)	3.67 m	3.60 dd (12.0, 6.0)
3″,5″-OCH_3	3.73 s	3.73 s	3.80 s	3.79 s	3.80 s	3.79 s	3.75 s

[a]Data (δ_H) were measured for **1**−**7** at 600 MHz. Coupling constants (J) in Hz are given in parentheses. The assignments were based on DEPT, $^1H-^1H$ COSY, HSQC, and HMBC experiments.

Table 2 ^{13}C NMR spectroscopic data for compounds **1**–**7** in CD_3OD[a].

No.	1	2	3	4	5	6	7
2	113.1	112.9	133.7	132.9	133.6	132.8	121.6
3	138.7	138.8	133.0	133.8	133.1	133.9	122.2
3a	122.3	122.2	122.8	122.7	122.7	122.8	118.6
4	119.0	119.0	118.6	118.7	118.7	118.8	153.5
5	119.8	119.8	119.7	119.7	119.6	119.6	103.4
6	122.9	122.9	121.9	122.0	121.9	121.9	123.0
7	111.1	111.0	111.9	111.9	111.9	111.9	106.7
7a	135.1	135.1	134.7	134.6	134.7	134.6	140.2
1′	56.0	55.9	35.6	35.7	35.5	35.6	38.2
2′	22.0	22.0	20.7	21.0	20.6	20.9	24.2
1″	135.4	135.4	137.4	137.2	137.2	137.2	141.5
2″	104.5	104.5	105.9	106.1	105.9	106.1	106.0
3″	149.3	149.3	149.1	149.1	149.1	149.1	148.8
4″	135.8	135.8	134.8	134.9	134.8	134.9	134.0
5″	149.3	149.3	149.1	149.1	149.1	149.1	148.8
6″	104.5	104.5	105.9	106.1	105.9	106.1	106.0
1‴	105.9	105.9	107.4	107.7	105.0	105.3	101.6
2‴	75.1	75.1	75.4	75.4	72.6	72.6	75.2
3‴	78.1	78.1	78.2	78.2	73.2	73.4	78.7
4‴	71.6	71.7	71.5	71.4	68.8	68.7	71.6
5‴	78.2	78.3	77.9	77.9	75.4	75.4	78.1
6‴	62.7	62.7	62.6	62.5	63.1	62.9	62.7
3″,5″-OCH_3	56.8	56.7	56.8	56.8	56.8	56.8	56.8

[a]Data (δ_C) were measured in for **1**–**7** at 150 MHz. The assignments were based on DEPT, ^{1}H–^{1}H COSY, HSQC, and HMBC experiments.

to the above units (Table 2). The presence of the β-glucopyranosyl unit was confirmed by enzymatic hydrolysis of **1** with snailase. The sugar isolated from the hydrolysate exhibited retention factor (R_f) on TLC, specific rotation {$[\alpha]_D^{20}$ +40.2 (*c* 0.08, H_2O)}, and ^{1}H NMR spectroscopic data identical to those of an authentic glucopyranose (see Experimental Section and Supporting Information Figs. S120 and S124).

As compared with those of the previously reported compounds from *I. indigotica*[40–55], the above spectroscopic data suggested that **1** was an unusual indole alkaloid β-D-glucoside containing the 1′-(4″-hydroxy-3″,5″-dimethoxyphenyl)ethyl moiety[56]. The structure was further elucidated by 2D NMR data analysis. In the ^{1}H–^{1}H COSY spectrum of **1**, homonuclear vicinal coupling cross-peaks of H-4/H-5/H-6/H-7 (Fig. 2), combined with the chemical shifts and coupling constants of these protons, confirmed the presence of the *ortho*-disubstituted benzene ring. In the HMBC spectrum, two and three-bond correlations from H-7 to C-3a and C-5; from H-4 to C-7a and C-6; from H-5 to C-7 and C-3a; from H-6 to C-4 and C-7a; and from H-2 to C-3, C-7a, and C-3a; along with their chemical shifts, proved that there was a 3-substituted indole moiety in **1**. The HMBC correlations from H-1‴ to C-3, combined with the ^{1}H–^{1}H COSY correlations of H-1‴/H-2‴/H-3‴/H-4‴/H-5‴/H_2-6‴ (Fig. 2) as well as chemical shifts of these proton and carbon resonances, located a β-D-glucopyranosyloxy unit at the C-3 of the indole moiety. In addition, the HMBC correlations from H-1′ to C-2, C-2′, C-2″/6″, and C-7a; from H_3-2′ to C-1′ and C-1″; along with the ^{1}H–^{1}H COSY cross-peaks between H-1′ and H_3-2′ and their chemical shifts, located the 1′-(4″-hydroxy-3″,5″-dimethoxyphenyl)ethyl moiety at the N atom of the indole moiety. Accordingly, the planar structure of **1** was elucidated as shown. The CD (circular dichroism) spectrum of **1** displayed two positive Cotton effects at 206 and 292 nm and a

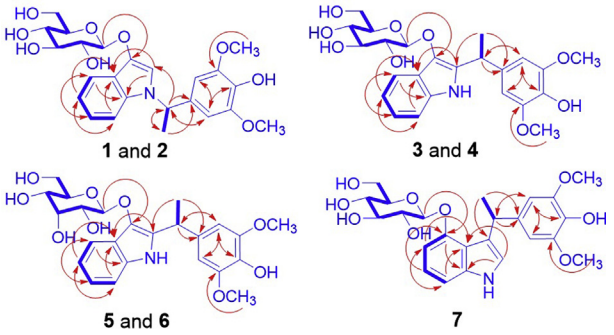

Figure 2 Main ^{1}H–^{1}H COSY (thick lines) and three-bond HMBC (arrows, from ^{1}H to ^{13}C) correlations of compounds **1**–**7**.

negative Cotton effect at 234 nm, arising from overlapped transitions of the indole and benzene chromophores[57] in the molecule. The 1′*S* configuration of **1** was assigned by calculations of ECD (electronic circular dichroism) spectra using the time-dependent density functional theory (TDDFT) method[58]. The calculated ECD spectrum of **1** was in well agreement with the experimental CD spectrum (Supporting Information Fig. S3). Therefore, the structure of compound **1** was determined and named isatidifoliumoside A.

Compound **2**, white amorphous powder {$[\alpha]_D^{20}$ −50.5 (*c* 0.1, MeOH)}, was separated by chiral HPLC from a mixture of **1** and **2** with peak integrations in around 1:1 ratio (Supporting Information Fig. S26). Comparison of the NMR spectroscopic data of **2** and **1** (Tables 1 and 2) demonstrated that the C-2 resonance in **2** was shielded by $\Delta\delta_C$ −0.2 ppm, while the other proton and carbon resonances were shifted by $\Delta\delta_H \leq \pm 0.01$ and $\Delta\delta_C \leq \pm 0.1$ ppm, respectively. This suggested that **2** was the 1′-epimer of **1**, which was confirmed by HR-ESI-MS and 2D NMR data analysis (Fig. 2) as well as by the specific rotation and CEs (Fig. 3) of **2**. Especially, the experimental CD and calculated ECD spectra of **2** were consistent with each other (Fig. S3). Thus, the structure of compound **2** was determined and named epiisatidifoliumoside A.

Compound **3**, a white amorphous powder with $[\alpha]_D^{20}$ +4.7 (*c* 0.1, MeOH), is another isomer of **1** as indicated by (+)-HR-ESI-MS, NMR, and IR spectroscopic data. Comparison of the NMR data of **3** with those of **1** (Tables 1 and 2) indicated that the two compounds mainly differed in substitution of the methine unit (C-2) in **1** by a quaternary carbon (δ_C 133.0) in **3**. In addition, as compared with those of **1**, the H-1′ and C-1′ resonances in **3** were shielded by $\Delta\delta_H$ −0.86 and $\Delta\delta_C$ −20.4 ppm. This suggested that the 1′-(4″-hydroxy-3″,5″-dimethoxyphenyl)ethyl moiety at the N atom in **1** was migrated to C-2 in **3**. The suggestion was verified by 2D NMR data analysis (Fig. 2). Especially the HMBC correlation from H-1‴ to C-3, from H-1′ to C-2, C-1″ and C-2″/6″, and from H-2′ to C-2 and C-1″ proved the locations of the β-glucopyranosyloxy and 1′-(4″-hydroxy-3″,5″-dimethoxyphenyl)ethyl moieties at C-3 and C-2 in **3**, respectively. Using the aforementioned protocol, the D-configuration of β-glucopyranosyl in **3** was verified. Comparison of the experimental CD and calculated ECD spectra supported the 1′*R* configuration of **3** (Supporting Information Fig. S6). Therefore, the structure of compound **3** was determined and named isatidifoliumoside B.

Compound **4**, a white amorphous powder with $[\alpha]_D^{20}$ −22.4 (*c* 0.1, MeOH), showed similar spectroscopic data as those of **3**. Comparison of the NMR spectroscopic data of the two compounds (Tables 1 and 2) demonstrated that H-2″/6″, H-6‴a and H-6‴b,

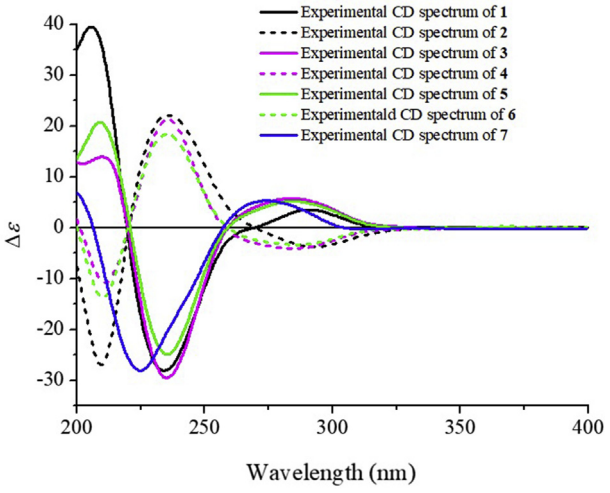

Figure 3 The overlaid experimental CD spectra of **1**−**7**.

and C-2 in **4** were shielded by $\Delta\delta_H$ −0.07, −0.16 and −0.07, and $\Delta\delta_C$ −0.8 ppm, respectively, whereas C-3 was deshielded by $\Delta\delta_C$ +0.8 ppm. This, together with nearly opposite CEs of the two compounds (Fig. 3), suggested that **4** was 1′-epimer of **3**, which was further confirmed by 2D NMR data analysis (Fig. 2) as well as by comparison of the experimental CD and calculated ECD spectra of **4** (Fig. S6). Thus, the structure of compound **4** was determined and named epiisatidifoliumoside B.

Compound **5**, a white amorphous powder with $[\alpha]_D^{20}$ +8.6 (*c* 0.1, MeOH), is the isomer of **3** and **4** having a different sugar unit, as indicated by spectroscopic data and confirmed by 2D NMR data analysis. Especially, in the HMBC spectrum, correlations from H-1‴ to C-3 and from H-2′ to C-2 (Fig. 2) confirmed that the sugar and 1′-(4″-hydroxy-3″,5″-dimethoxyphenyl)ethyl units located at C-3 and C-2 of the indole nucleus in **5**, respectively. In the ^{1}H NMR spectrum of **5**, the coupling constants ($J_{1‴,2‴}$ = 7.8 Hz, $J_{2‴,3‴} = J_{3‴,4‴}$ = 3.0 Hz, and $J_{4‴,5‴}$ = 9.6 Hz) indicated that the sugar unit was *β*-allopyranosyl only differing from *β*-glycopyranosyl in the 3‴-configuration. This deduction was proved by enzymatic hydrolysis of **5** with snailase. The sugar isolated from the hydrolysate of **5** exhibited retention factor (R_f) on TLC, specific rotation {$[\alpha]_D^{20}$ +12.0 (*c* 0.07, H_2O)} (see Experimental Section), and ^{1}H NMR spectroscopic data completely identical to those of an authentic D-allopyranose (Supporting Information Figs. S122 and S125). Similarity of the CD curves between **5** and **3** (Fig. 3) demonstrated that the two compounds possessed the same 1′*R* configuration, which was supported by comparison of the experimental CD and the calculated ECD spectra of **5** (Supporting Information Fig. S9). Therefore, the structure of compound **5** was determined and named isatidifoliumoside C.

Compound **6** was obtained as a white amorphous powder with $[\alpha]_D^{20}$ −35.6 (*c* 0.1, MeOH). Comparison of the NMR spectroscopic data of **6** and **5** (Tables 1 and 2) demonstrated that the H-6‴a and H-6‴b, and C-2 resonances in **6** were shielded by $\Delta\delta_H$ −0.16, −0.07 and $\Delta\delta_C$ −0.8 ppm, respectively, whereas the C-3 resonance was deshielded by $\Delta\delta_C$ +0.8 ppm. The differences suggested that **6** is the 1′-epimer of **5**, which was supported by the reverse CEs in the CD spectrum of **6** as compared with that of **5** (Fig. 3). The elucidation was verified by 2D NMR data analysis (Fig. 2) as well as by consistence of the experimental CD and calculated ECD spectra of **6** (Fig. S9). Thus, the structure of compound **6** was determined and named epiisatidifoliumoside C.

Compound **7** was obtained as a white amorphous powder with $[\alpha]_D^{20}$ −67.5 (*c* 0.1, MeOH). The spectroscopic data demonstrated that **7** was one more isomer of **3** and **4** having the same *β*-D-glucopyranosyl unit. The presence of *β*-D-glucopyranosyl in **7** was verified by enzymatic hydrolysis (see Experimental Section). As compared, the NMR spectroscopic data (Tables 1 and 2) indicated replacement of the 2,3-disubstited indole nucleus in **3** and **4** by a 3,4-disubstited indole in **7**. This was confirmed by 2D NMR spectroscopic data analysis of **7** (Fig. 2). In particular, the HMBC spectrum of **7** showed the correlations from H-1′ to C-1″, C-2, C-3, C-3a, and C-2″/6″; from H-1‴ to C-4; and from H_3-2′ to C-1″ and C-3. These correlations revealed that the *β*-D-glucopyranosyloxy and 1′-(4″-hydroxy-3″,5″-dimethoxyphenyl)ethyl units substituted at the C-4 and C-3 of the indole nucleus in **7**, respectively. The 1′*S* configuration of **7** was assigned by consistence of the experimental CD and calculated ECD spectra (Supporting Information Fig. S12). Therefore, the structure of **7** was determined and named isatidifoliumoside D.

Adducting and deducting analysis of the specific rotation data of the three pairs of epimers showed that the glycosidic indole moieties contributed the $[\alpha]_D^{20}$ values of −37.1, −8.9, and −13.4 to **1/2**, **3/4**, and **5/6**, respectively, while the (1′*S*)-/(1′*R*)-1′- and (1′*R*)-/(1′*S*)-1′-(4″-hydroxy-3″,5″-dimethoxyphenyl)ethyl unit contributed +/−13.4 to **1/2** and +/−13.5 and +/−22.0 to **3/4** and **5/6**. These data revealed that the contributions of the 1′-(4″-hydroxy-3″,5″-dimethoxyphenyl)ethyl unit to the specific rotation data depended upon the C-1′ configuration as well as the location of the unit at the glycosidic indole nucleus. At the N-1 atom, the (1′*S*)-1′-(4″-hydroxy-3″,5″-dimethoxyphenyl)ethyl had the positive contribution (**1**), and at C-2 (**4** and **6**) the negative. In contrast, (1′*R*)-1′-(4″-hydroxy-3″,5″-dimethoxyphenyl)ethyl at N-1 (**2**) had the negative contribution, and at C-2 (**3** and **5**) the positive. As compared with those of **1**, **2**, **4**, and **6**, the specific rotation value of **7** suggested that the (1′*S*)-1′-(4″-hydroxy-3″,5″-dimethoxyphenyl)ethyl unit at C-3 had the negative contribution though the 1′*R* epimer of **7** was not obtained in this study. In addition, comparison of the CD spectra of **1**−**6** showed that signs of the CEs were dominated by the C-1′ configuration and location of the 1′-(4″-hydroxy-3″,5″-dimethoxyphenyl)ethyl unit (Fig. 3). The CD spectra of **1**−**6** display three CEs around 210, 236, and 288 nm, arising from the overlapped $^1B_a/^1L_a$, $^1B_b/^1L_b$, and ^1L_b/transitions of the substituted indole/benzene chromophores[57], respectively. The (1′*S*)-1′-(4″-hydroxy-3″,5″-dimethoxyphenyl)ethyl unit at the N atom (**1**) dominated the positive $^1B_a/^1L_a$ (210 nm) and ^1L_b/(293 nm) and negative $^1B_b/^1L_b$ (236 nm) CEs, whereas at C-2 (**4** and **6**) it gave the corresponding reverse CEs. Meanwhile, the (1′*R*)-1′-(4″-hydroxy-3″,5″-dimethoxyphenyl)ethyl unit at the N atom (**2**) dominated the negative $^1B_a/^1L_a$ and ^1L_b/and positive $^1B_b/^1L_b$ CEs, and at C-2 (**3** and **5**) the positive $^1B_a/^1L_a$ and ^1L_b/and negative$^1B_b/^1L_b$ CEs. Adduction of the CD data between the epimeric pairs indicated that the glycosidic indole moieties in **1**−**6** had the relatively weak contributions to the $^1B_a/^1L_a$ (positive) and ^1L_b (negative) CEs. This was supported by high consistence of the experimental CD and calculated ECD spectra of **1**−**6** (Figs. S3, S6, and S9) as well as by the calculated ECD spectra of aglycones **1a**−**6a** (Supporting Information Figs. S14, S16, and S17) and the proposed biogenetic precursors **8** and **9** (Supporting Information Figs. S23−25). The CD spectrum of **7** exhibited the positive $^1B_a/^1L_a$ (200 nm) and ^1L_b/(274 nm) and negative $^1B_b/^1L_b$ (225 nm) CEs. As compared with those of **3** and **4**, wavelengths of the CE maximums of **7** were blue-shifted by $\Delta\lambda_{max}$ 10 nm (see Fig. 3), which would be due to the location change of the substituents at the indole ring. Further comparison of the

experimental CD and calculated ECD spectra supported that the 1′*S* configuration dominated the CEs of **7**. This was also supported by the calculated ECD spectra of the aglycone **7a** and the proposed biogenetic precursor **10** (Supporting Information Figs. S19 and S25).

Based on the above analysis, two preliminary rules to assign location and configuration of the *β*-D-glucopyranosyloxy, *β*-D-allopyranosyloxy, and 1′-(4″-hydroxy-3″,5″-dimethoxyphenyl)ethyl in these indole glycosides are disclosed: (a) *β*-D-glucopyranosyloxy at C-3 or C-4 as well as *β*-D-allopyranosyloxy at C-3 of the indole nucleus have the negative contributions to both the specific rotation ($[\alpha]_D^{20}$>8.0) and ^1B_b CE (230 ± 7 nm); and (b) the (1′*S*)-1′-(phenyl) ethyl units at the N atom or C-3 and the (1′*R*)-1′-(phenyl)ethyl units at C-2 positively contributes to the specific rotation and ^1L_b/CE (284 ± 10 nm) but negatively to the $^1B_b/^1L_b$ (230 ± 7 nm) CE, whereas the (1′*R*)-1′-(phenyl)ethyl units at the N atom or C-3 and the (1′*S*)-1′-(phenyl)ethyl units at C-2 negatively contributes to the specific rotation and ^1L_b/CE (284 ± 10 nm) but positively to the $^1B_b/^1L_b$ (230 ± 7 nm) CE. The roles simply using the specific rotation and/or CD data may be validated to determination of the location and configuration of other *β*-glycopyranosyloxy and 1′-(phenyl)ethyl units in the related indole glycosides.

Compounds **1**−**7**, together with isatidifoliumindolinones A−D from the same extract[56], represent the first examples of natural products with the novel carbon skeleton derived from coupling between the indole or indolin-3-one and phenylethyl units, especially **1**−**7** are the first glycosidic forms. Based on the molecular architecture, the biosynthetic precursors of **1**−**7** are traced to 1*H*-indol-3-ol glycosides (**8**−**10**) and sinapic acid (**11**), among them **8** was reported from the roots of the plant[42] and **11** from this study. A plausible biosynthetic pathway for **1**−**7** is postulated in Scheme 1. Decarboxylation of **11** gives an intermediate 2,6-dimethoxy-4-vinylphenol (**12**), which undergoes nucleophilic addition with **8**, **9**, or **10** to generate **1**−**7**. Interestingly, in this plant the epimers occur in the relative ratios of 1:1 for **1/2** and 3:2 for **3/4** and **5/6**, as indicated by chiral HPLC separation (Supporting Information Figs. S26−28). This demonstrates that the nucleophilic addition of **12** with **8** to produce **1/2** is non-stereoselective, while the addition of **12** with **8** or **9** to give **3/4** or **5/6** is partially stereoselective. However, the addition of **12** with **10** to yield **7** is fully stereoselective. These facts suggest that location of *β*-D-glucopyranosyloxy/*β*-D-allopyranosyloxy and nucleophilic center on the indole nucleus play important roles in stereoselective biosynthesis of **1**−**7**. In addition, **3** and/or **4** is the potential precursors of isatidifoliumindolinones A−D[56] that may be produced by hydrolysis of **3** and/or **4**, followed by successive or simultaneous oxidation and methylation/methoxylation (not shown in Scheme 1).

In the preliminary *in vitro* assays, compounds **3** and **4** as well as their mixture in 1:1 showed inhibitory activity against the K^+ channel KCNQ2 in CHO cells with IC_{50} 19.15, 11.57, and 13.27 μmol/L, respectively (the positive control ML252, IC_{50} 0.27 ± 0.2 μmol/L), indicating that **4** with the 1′*S* configuration is relatively more active than **3** with the 1′*R* configuration. However, in this assay **1**, **2**, and **5**−**7** were inactive at a concentration of 10^{-4} mol/L. In addition, the mixture of **5** and **6** in the 3:2 ratio exhibited antiviral activity against influenza virus H1N1 PR8 with IC_{50} 64.7 μmol/L (the positive control ribavirin, IC_{50} 54.3 μmol/L), while the individual epimers **5** and **6** were inactive (10^{-4} mol/L). This suggested that the epimers had a synergistic effect against influenza virus H1N1 PR8. The results provide preliminary clues for activity−structure relationships of these indole glycosides. For KCNQ2 inhibition, *β*-D-glucopyranosyloxy at C-3 is required while the 1′*S* configuration may increase activity, and for anti-influenza virus H1N1 PR8, *β*-D-allopyranosyloxy at C-3 and a synergistic effect of the 1′*S* and 1′*R* configurations play roles.

3. Conclusions

Seven indole alkaloid glycosides containing the 1′-(4″-hydroxy-3″,5″-dimethoxyphenyl)ethyl unit (**1**−**7**) were isolated from the *I.*

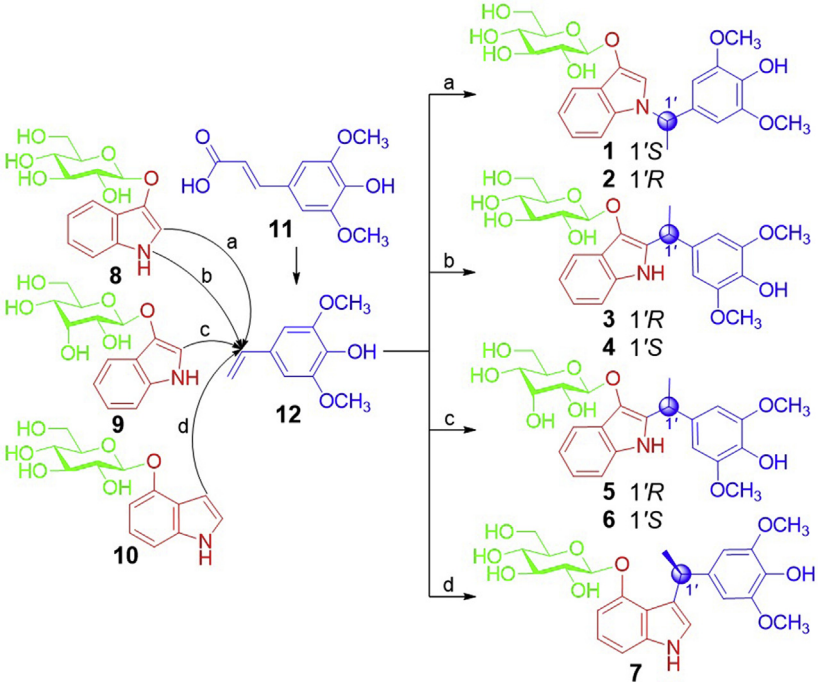

Scheme 1 Proposed biosynthetic pathways of **1**−**7**.

indigotica leaves (da qing ye) decoction. The aglycones, together with that of the stereoisomer isatidifoliumindolinones A−D from the same decoction[56], represent a novel group of the indole alkaloid natural products. Based on structure-specific rotation/Cotton effect analysis of **1**−**7**, two preliminary roles are proposed for assignment of the location and configuration of the β-glycopyranosyloxy and 1′-(phenyl)ethyl units in the indole alkaloid glycosides. Compounds **5** and **6** are the first indole alkaloid β-D-allopyranosides. Especially the two allopyranoside epimers showed the synergistic effect against influenza virus H1N1 PR8, representing the novel antiviral constituents from the decoction of *I. indigotica* leaves[9,23,59] that support clinical application of the herbal medicine and the theory of multiple active components of traditional Chinese medicine.

4. Experimental

4.1. General experimental procedures

See Supporting Information.

4.2. Plant material

See Ref.[56].

4.3. Extraction and isolation

For preliminary extraction and isolation, see Ref. 56. Subfraction B2-4-1-21 (1.5 g) was chromatographed over silica gel, eluting with $CHCl_2$/MeOH (15:1), to give B2-4-1-21-1−B2-4-1-21-10, of which B2-4-1-21-8 (60 mg) was further separated by RP-HPLC (25% acetonitrile, 3.0 mL/min) to afford a mixture (20 mg, t_R = 35.1 min). The mixture was separated by chiral HPLC with a Chiralpak AD-H column (250 mm × 10 mm) using a mobile phase of EtOH/*n*-hexane (27:73, flow rate 1.0 mL/min) to yield **5** (5.0 mg, t_R = 34.1 min) and **6** (3.5 mg, t_R = 37.8 min). Subfraction B2-4-2-9 (500 mg) was further fractionated by CC over HW-40C (MeOH) to yield B2-4-2-9-1−B2-4-2-9-4, of which subfraction B2-4-2-9-2 (16 mg) was separated by RP-HPLC (40% MeOH, 3.0 mL/min) afforded **7** (4.0 mg, t_R = 25.0 min). Fraction B2-4-2 (20 g) was fractionated by CC over RP (C18) silica gel (460 mm × 36 mm, 150 g) eluting with a gradient of increasing MeOH concentration (0%−100%) in H_2O to yield B2-4-2-1−B2-4-2-28. Purification of B2-4-2-25 (30 mg) by RP-HPLC (8% acetonitrile, 3.0 mL/min) afforded a mixture (12 mg, t_R = 22.2 min), which was further separated by chiral HPLC with a Chiralpak AD-H column (250 mm × 10 mm, EtOH/*n*-hexane 3:7, flow rate 1.5 mL/min) to obtain **1** (4.0 mg, t_R = 22.3 min) and **2** (3.5 mg, t_R = 37.2 min). Separation of B2-4-2-19 (300 mg) by RP-HPLC (30% MeOH, 3.0 mL/min) afforded the mixture (10 mg, t_R = 77.0 min), which were isolated by chiral HPLC with a Chiralpak AD-H column (250 mm × 10 mm, EtOH/*n*-hexane 1:3, flow rate 2.5 mL/min) to obtain **3** (4.5 mg, t_R = 30.6 min) and **4** (3.0 mg, t_R = 35.7 min).

4.3.1. Isatidifoliumoside A (*1*)

White amorphous powder; $[\alpha]_D^{20}$ −23.7 (*c* 0.1, MeOH); UV (MeOH) λ_{max} (log ε) 207 (4.59), 228 (4.40), 281 (3.64) nm; CD (MeOH) λ_{max} ($\Delta\varepsilon$) 206 (+39.5), 234 (−28.1), 292 (+3.53) nm; IR ν_{max} 3403, 2935, 1613, 1554, 1519, 1460, 1427, 1361, 1331, 1225, 1157, 1115, 911, 836, 800, 743, 670, 615 cm^{-1}; see ^1H NMR (CD_3OD, 600 MHz) data in Table 1; See ^{13}C NMR (CD_3OD, 150 MHz) data in Table 2; (+)-ESI-MS *m/z* 476 $[M+H]^+$, 498 $[M+Na]^+$; (−)-ESI-MS *m/z* 474 $[M-H]^-$; (+)-HR-ESI-MS *m/z* 498.1746 $[M+Na]^+$ (Calcd. for $C_{24}H_{29}NO_9Na$, 498.1735).

4.3.2. Episatidifoliumoside A (*2*)

White amorphous powder; $[\alpha]_D^{20}$ −50.5 (*c* 0.1, MeOH); UV (MeOH) λ_{max} (log ε) 207 (4.74), 228 (4.54), 281 (3.84) nm; CD (MeOH) λ_{max} ($\Delta\varepsilon$) 210 (−26.9), 236 (+22.1), 293 (−3.73) nm; IR ν_{max} 3402, 2934, 1613, 1554, 1519, 1460, 1427, 1361, 1331, 1226, 1157, 1116, 911, 836, 800, 743, 670, 614 cm^{-1}; see ^1H NMR (CD_3OD, 600 MHz) data in Table 1; see ^{13}C NMR (CD_3OD, 150 MHz) data in Table 2; (+)-ESI-MS *m/z* 498 $[M+Na]^+$; (−)-ESI-MS *m/z* 474 $[M-H]^-$; (+)-HR-ESI-MS *m/z* 498.1739 $[M+Na]^+$ (Calcd. for $C_{24}H_{29}NO_9Na$, 498.1735).

4.3.3. Isatidifoliumoside B (*3*)

White amorphous powder; $[\alpha]_D^{20}$ +4.7 (*c* 0.1, MeOH); UV (MeOH) λ_{max} (log ε) 206 (4.67), 227 (4.40), 283 (3.85) nm; CD λ_{max} ($\Delta\varepsilon$) 210 (+13.9), 235 (−29.5), 284 (+5.78) nm; IR ν_{max} 3359, 2971, 2932, 1701, 1617, 1518, 1459, 1427, 1326, 1220, 1157, 1115, 1072, 941, 901, 838, 797, 750, 588 cm^{-1}; see ^1H NMR (CD_3OD, 600 MHz) data in Table 1; see ^{13}C NMR (CD_3OD, 150 MHz) data in Table 2; (+)-ESI-MS *m/z* 498 $[M+Na]^+$; (−)-ESI-MS *m/z* 474 $[M-H]^-$; (+)-HR-ESI-MS *m/z* 476.1922 $[M+H]^+$ (Calcd. for $C_{24}H_{30}NO_9$, 476.1915).

4.3.4. Episatidifoliumoside B (*4*)

White amorphous powder; $[\alpha]_D^{20}$ −22.4 (*c* 0.1, MeOH); UV (MeOH) λ_{max} (log ε) 206 (4.51), 226 (4.38), 281 (3.79) nm; CD λ_{max} ($\Delta\varepsilon$) 211 (−10.8), 236 (+22.3), 284 (−4.11) nm; IR ν_{max} 3352, 2972, 2931, 1702, 1616, 1518, 1459, 1426, 1326, 1220, 1116, 1075, 1047, 941, 880, 837, 798, 749, 636 cm^{-1}; see ^1H NMR (CD_3OD, 600 MHz) data in Table 1; see ^{13}C NMR (CD_3OD, 150 MHz) data in Table 2; (+)-ESI-MS *m/z* 498 $[M+Na]^+$; (−)-ESI-MS *m/z* 474 $[M-H]^-$; (+)-HR-ESI-MS *m/z* 476.1925 $[M+H]^+$ (Calcd. for $C_{24}H_{30}NO_9$, 476.1915).

4.3.5. Isatidifoliumoside C (*5*)

White amorphous powder; $[\alpha]_D^{20}$ +8.6 (*c* 0.1, MeOH); UV (MeOH) λ_{max} (log ε) 206 (4.57), 226 (4.55), 282 (4.01) nm; CD λ_{max} ($\Delta\varepsilon$) 210 (+20.7), 236 (−24.8), 285 (+5.24) nm; IR ν_{max} 3373, 2932, 1616, 1518, 1459, 1426, 1326, 1218, 1115, 1041, 941, 910, 837, 797, 735, 633 cm^{-1}; see ^1H NMR (CD_3OD, 600 MHz) data in Table 1; see ^{13}C NMR (CD_3OD, 150 MHz) data in Table 2; (+)-ESI-MS *m/z* 498 $[M+Na]^+$; (+)-HR-ESI-MS *m/z* 476.1929 $[M+H]^+$ (Calcd. for $C_{24}H_{30}NO_9$, 476.1915).

4.3.6. Episatidifoliumoside C (*6*)

White amorphous powder; $[\alpha]_D^{20}$ −35.6 (*c* 0.1, MeOH); UV (MeOH) λ_{max} (log ε) 206 (4.62), 227 (4.37), 282 (3.77) nm; CD λ_{max} ($\Delta\varepsilon$) 210 (−13.7), 236 (+18.4), 287 (−3.37) nm; IR ν_{max} 3375, 2927, 1966, 1616, 1518, 1459, 1426, 1325, 1218, 1115, 1039, 941, 910, 837, 797, 736 cm^{-1}; see ^1H NMR (CD_3OD, 600 MHz) data in Table 1; see ^{13}C NMR (CD_3OD, 150 MHz) data in Table 2; (+)-ESI-MS *m/z* 498 $[M+Na]^+$; (−)-ESI-MS *m/z* 474 $[M-H]^-$; (+)-HR-ESI-MS *m/z* 476.1928 $[M+H]^+$ (Calcd. for $C_{24}H_{30}NO_9$, 476.1915).

4.3.7. Isatidifoliumoside D (*7*)

White amorphous powder; $[\alpha]_D^{20}$ −67.5 (*c* 0.1, MeOH); UV (MeOH) λ_{max} (log ε) 206 (4.68), 222 (4.62), 271 (3.93) nm; CD λ_{max} ($\Delta\varepsilon$) 225 (−28.1), 274 (+5.33) nm; IR ν_{max} 3370, 2968,

2934, 1677, 1617, 1514, 1460, 1426, 1356, 1325, 1229, 1079, 913, 838, 800, 743, 655 cm^{-1}; see ^1H NMR (CD_3OD, 600 MHz) data in Table 1; see ^{13}C NMR (CD_3OD, 150 MHz) data in Table 2; (+)-ESI-MS *m/z* 498 $[M+Na]^+$; (−)-ESI-MS *m/z* 474 $[M-H]^-$; (+)-HR-ESI-MS *m/z* 498.1726 $[M+Na]^+$ (Calcd. for $C_{24}H_{29}NO_9Na$ 498.1735).

4.3.8. *Enzymatic hydrolysis of **1**, **3**, **5**, and **7***

Compounds **1**, **3**, **5**, and **7** (2.0−3.0 mg) were separately hydrolyzed in H_2O (5 mL) with snailase (5.0 mg, CODE S0100, Beijing Biodee Biotech Co., Ltd., Beijing, China) at 37 °C for 24 h. The hydrolysate was evaporated under reduced pressure, then chromatographed over silica gel eluting with CH_3CN/H_2O (8:1), to yield sugar. The sugar (0.8−1.2 mg) from the hydrolysates of **1**, **3**, and **7** gave retention factor (R_f ~0.41) on TLC (CH_2Cl_2/MeOH/H_2O, 7:3.5:1), $[\alpha]_D^{20}$ +36.5−+40.2 (*c* 0.06−0.08, H_2O), and ^1H NMR (D_2O, 600 MHz) data, consistent with those of the authentic D-glucose (Figs. S120, S121, S123, and S124). The sugar (0.7 mg) from the hydrolysate of **5** gave retention factor (R_f ~0.47) on TLC (CH_2Cl_2/MeOH/H_2O, 7:3.5:1), $[\alpha]_D^{20}$ +12.0 (*c* 0.07, H_2O), and ^1H NMR (D_2O, 600 MHz) data, consistent with those of the authentic D-allose (Figs. S122 and S125).

4.3.9. *ECD calculations of **1**−**10** and aglycones **1a**−**7a***

For details, see Supporting Information. Briefly, conformational analysis was conducted by Monte Carlo searching with the MMFF94 molecular mechanics force field using the Molecular Operating Environment (MOE) software for **1**−**6** and Gaussian 16 program package for **7**, **1a**−**7a**, and **8**−**10**. The lowest-energy conformers having relative energies within 3 kcal/mol were optimized with the Gaussian 09 or Gaussian 16 program. Subsequently, the conformers were re-optimized using DFT at the B3LYP/6-31 + G (d, p) level for **1**−**7** and at APFD/6-31 + G (d, p) for **8**−**10** and aglycones **1a**−**7a**, with the solvent effects considered using the dielectric constant of MeOH (ε = 32.6) *via* conductor-like polarizable continuum model (CPCM). The energies, oscillator strengths, and rotational strengths of the excitations were calculated using the TDDFT methodology at the B3LYP/6−311++G (2d, 2p) level in vacuum for **1**−**7** and at APFD/6-311 + G (2d, p) for **8**−**10** and aglycones **1a**−**7a**. The re-optimized conformers showed relative Gibbs free energies (ΔG) under 3 kcal/mol were used for ECD spectra simulation. The ECD spectra were simulated by the Gaussian function (σ = 0.28 eV). To obtain the final spectra, the simulated spectra of the lowest energy conformers were averaged on the basis of the Boltzmann distribution theory and their relative Gibbs free energy (ΔG).

Acknowledgments

Financial support of the National Natural Science Foundation of China (81630094, 21732008, and 81730093), CAMS Innovation Fund for Medical Science of China (2017-I2M-3-010 and 2016-I2M-1-010), and the Drug Innovation Major Project (2018ZX09711001-001-001, China) is acknowledged.

Author contributions

Jiangong Shi designed and guided all the chemical experiments, analyzed the data, and rewrote and revised the manuscript. Qinglan Guo and Dawei Li conducted the chemical experiments, doublechecked the data, and wrote the preliminary manuscript. Ying Guo, Haibo Yu, and Xiaoliang Wang designed the pharmacological test and analyzed the corresponding data. Chengbo Xu and Chenggen Zhu assisted the chemical experiments. All authors read and approved the final manuscript.

Conflicts of interest

The authors have no conflicts of interest to declare.

Appendix A. Supporting information

Supporting data to this article can be found online at https://doi.org/10.1016/j.apsb.2019.09.001.

References

1. Jiangsu New Medical College. *Dictionary of traditional Chinese medicine*, Vol. 1. Shanghai: Shanghai Science and Technology Publishing House; 1986. p. 126−1250.
2. Huang QS, Yoshihira K, Natori S. Isolation of 2-hydroxy-3-butenyl thiocyanate, epigoitrin, and adenosine from "banlangen", *Isatis indigotica* Root. *Planta Med* 1981;**42**:308−10.
3. Wu X, Liu Y, Sheng W, Sun J, Qin G. Chemical constituents of *Isatis indigotica*. *Planta Med* 1997;**63**:55−7.
4. Wu X, Qin G, Cheung KK, Cheng K. New alkaloids from *Isatis indigotica*. *Tetrahedron* 1997;**53**:13323−8.
5. Li B, Chen WS, Zheng SQ, Yang GJ, Qiao CZ. Two new alkaloids isolated from tetraploidy banlangen. *Acta Pharm Sin* 2000;**35**:508−10.
6. Chen WS, Li B, Zhang WD, Yang GJ, Qiao CZ. A new alkaloid from the root of *Isatis indigotica* Fort. *Chin Chem Lett* 2001;**12**:501−2.
7. Liu HL, Wu LJ, Li H, Wang J. Study on the chemical constituents of *Isatis indigotica* fort. *J Shenyang Pharm Univ* 2002;**19**:93−5. 100.
8. He Y, Lu J, Lin RC. Studies on chemical constituents in root of *Isatis indigotica*. *Chin Tradit Herb Drugs* 2003;**34**:777−8.
9. Mark NK, Leung CY, Wei XY, Shen XL, Wong RN, Leung KN, et al. Inhibition of RANTES expression by indirubin in influenza virus-infected human bronchial epithelial cells. *Biochem Pharmacol* 2004;**67**:167−74.
10. Wei XY, Leung CY, Wong CK, Shen XL, Wong RN, Cai ZW, et al. Bisindigotin, a TCDD antagonist from the Chinese medicinal herb *Isatis indigotica*. *J Nat Prod* 2005;**68**:427−9.
11. Li B, Chen WS, Zhao Y, Zhang HM, Dong JX, Qiao CZ. Phenylpropanoids isolated from tetraploid roots of *Isatis indigotica*. *Chin Tradit Herb Drugs* 2005;**36**:326−8.
12. Ruan JL, Zou JH, Cai YL. Studies on chemical constituents in leaf of *Isatis indigotica*. *China J Chin Mater Med* 2005;**30**:1525−6.
13. Liu R, Yuan B, Liu Z, Li X, Xiong Z, Li F. Identification of 5 constituents of the aqueous extract of *Isatis indigotica* by HPLC−MS^2. *J Chin Med Mater* 2005;**28**:772−4.
14. He LW, Li X, Chen JW, Sun DD, Ju WZ, Wang KC. Chemical constituents from water extract of *Radix isatidis*. *Acta Pharm Sin* 2006;**41**:1193−6.
15. Liu JF, Zhang XM, Xue DQ, Jiang ZY, Gu Q, Chen JJ. Studies on chemical constituents from leaves of *Isatis indigotica*. *China J Chin Mater Med* 2006;**31**:1961−5.
16. He L, Li X, Chen J, Wu J, Sun D. Studies on water-soluble chemical constitutions in *Radix Isatidis*. *China Pharm* 2006;**17**:232−4.
17. Liu JF, Jiang ZY, Wang RR, Zheng YT, Chen JJ, Zhang XM, et al. Isatisine A, a novel alkaloid with an unprecedented skeleton from leaves of *Isatis indigotica*. *Org Lett* 2007;**9**:4127−9.
18. Bai J, Xiao H, He JW, Yan YX, Wang YS, Yang SL. Studies on chemical constituents from the root of *Isatis indigotica*. *China J Chin Mater Med* 2007;**32**:271−2.

19. Zuo L, Li JB, Xu J, Yang JZ, Zhang DM, Tong YL. Studies on chemical constituents in root of *Isatis indigotica*. *China J Chin Mater Med* 2007;**32**:688−91.
20. Sun DD, Dong WW, Li X, Zhang HQ. Isolation, structural determination and cytotoxic activity of two new ceramides from the root of *Isatis indigotica*. *Sci China Ser B Chem* 2009;**52**:621−5.
21. Sun DD, Dong WW, Li X, Zhang HQ. Indole alkaloids from the roots of *Isatis ingigotica* and their antiherpes simplex virus type 2 (HSV-2) activity *in vitro*. *Chem Nat Comp* 2010;**46**:763−6.
22. Wu Y, Zhang ZX, Hu H, Li D, Qiu G, Hu X, et al. Novel indole *C*-glycosides from *Isatis indigotica* and their potential cytotoxic activity. *Fitoterapia* 2011;**82**:288−92.
23. Yang Z, Wang Y, Zheng Z, Zhao S, Zhao J, Lin Q, et al. Antiviral activity of *Isatis indigotica* root-derived clemastanin B against human and avian influenza A and B viruses *in vitro*. *Int J Mol Med* 2013;**31**:867−73.
24. He LW, Dong W, Yang JY, Li X, Li W. Chemical constituents in antiviral fraction of Isatidis Radix and their activities. *Chin Tradit Herb Drugs* 2013;**44**:2960−4.
25. Yang L, Wang G, Wang M, Jiang H, Chen L, Zhao F, et al. Indole alkaloids from the roots of *Isatis indigotica* and their inhibitory effects on nitric oxide production. *Fitoterapia* 2014;**95**:175−81.
26. Jiang YP, Guo QL, Liu YF, Shi JG. Codonopiloneolignanin A, a polycyclic neolignan with a new carbon skeleton from the roots of *Codonopsis pilosula*. *Chin Chem Lett* 2016;**27**:55−8.
27. Jiang Y, Liu Y, Guo Q, Xu C, Zhu C, Shi J. Sesquiterpene glycosides from the roots of *Codonopsis pilosula*. *Acta Pharm Sin B* 2016;**6**:46−54.
28. Jiang YP, Liu YF, Guo QL, Xu CB, Lin S, Zhu CG, et al. Lignanoids from an aqueous extract of the roots of *Codonopsis pilosula*. *Acta Pharm Sin* 2016;**51**:616−25.
29. Guo QL, Lin S, Wang YN, Zhu CG, Xu CB, Shi JG. Gastrolatathioneine, an unusual ergothioneine derivative from an aqueous extract of "tian ma": a natural product co-produced by plant and symbiotic fungus. *Chin Chem Lett* 2016;**27**:1577−81.
30. Liu Z, Wang W, Feng N, Wang L, Shi J, Wang X. Parishin C′s prevention of Aβ_{1-42}-induced inhibition of long-term potentiation is related to NMDA receptors. *Acta Pharm Sin B* 2016;**6**:189−97.
31. Huang JY, Yuan YH, Yan JQ, Wang YN, Chu SF, Zhu CG, et al. 20C, a bibenzyl compound isolated from *Gastrodia elata*, protects PC12 cells against rotenone-induced apoptosis *via* activation of the Nrf2/ARE/HO-1 signaling pathway. *Acta Pharmacol Sin* 2016;**37**:731−40.
32. Liu ZH, Ma H, Wang WP, Xu SF, Wang L, Shi JG, et al. Structure−activity relationship of gastrodin and parishins on learning and memory deficits induced by scopolamine. *Acta Pharm Sin* 2016;**51**:743−8.
33. Zhou X, Guo QL, Zhu CG, Xu CB, Wang YN, Shi JG. Gastradefurphenol, a minor 9,9′-neolignan with a new carbon skeleton substituted by two *p*-hydroxybenzyls from an aqueous extract of "tian ma". *Chin Chem Lett* 2017;**28**:1185−9.
34. Zhang XL, Yuan YH, Shao QH, Wang ZZ, Zhu CG, Shi JG, et al. DJ-1 regulating PI3K-Nrf2 signaling plays a significant role in bibenzyl compound 20C-mediated neuroprotection against rotenone-induced oxidative insult. *Toxicol Lett* 2017;**271**:74−83.
35. Meng XH, Jiang ZB, Zhu CG, Guo QL, Xu CB, Shi JG. Napelline-type C_{20}-diterpenoid alkaloid iminiums from an aqueous extract of "fu zi": solvent-/base-/acid-dependent transformation and equilibration between alcohol iminium and aza acetal forms. *Chin Chem Lett* 2016;**27**:993−1003.
36. Meng XH, Jiang ZB, Guo QL, Shi JG. A minor arcutine-type C_{20}-diterpenoid alkaloid iminium constituent of "fu zi". *Chin Chem Lett* 2017;**28**:588−92.
37. Meng XH, Guo QL, Zhu CG, Shi JG. Unprecedented C_{19}-diterpenoid alkaloid glycosides from an aqueous extract of "fu zi": neoline 14-*O*-L-arabinosides with four isomeric L-anabinosyls. *Chin Chem Lett* 2017;**28**:1705−10.
38. Guo Q, Xia H, Meng X, Shi G, Xu C, Zhu C, et al. C_{19}-Diterpenoid alkaloid arabinosides from an aqueous extract of the lateral root of *Aconitum carmichaelii* and their analgesic activities. *Acta Pharm Sin B* 2018;**8**:409−19.
39. Guo Q, Xia H, Shi G, Zhang T, Shi J. Aconicarmisulfonine A, a sulfonated C_{20}-diterpenoid alkaloid from the lateral roots of *Aconitum carmichaelii*. *Org Lett* 2018;**20**:816−9.
40. Chen M, Gan L, Lin S, Wang X, Li L, Li Y, et al. Alkaloids from the root of *Isatis indigotica*. *J Nat Prod* 2012;**75**:1167−76.
41. Chen M, Lin S, Li L, Zhu C, Wang X, Wang Y, et al. Enantiomers of an indole alkaloid containing unusual dihydrothiopyran and 1,2,4-thiadiazole rings from the root of *Isatis indigotica*. *Org Lett* 2012;**14**:5668−71.
42. Wang XL, Chen MH, Wang F, Bu PB, Lin S, Zhu CG, et al. Chemical constituents from root of *Isatis indigotica*. *China J Chin Mater Med* 2013;**38**:1172−82.
43. Liu YF, Chen MH, Wang XL, Guo QL, Zhu CG, Lin S, et al. Antiviral enantiomers of a bisindole alkaloid with a new carbon skeleton from the roots of *Isatis indigotica*. *Chin Chem Lett* 2015;**26**:931−6.
44. Liu YF, Chen MH, Guo QL, Lin S, Xu CB, Jiang YP, et al. Antiviral glycosidic bisindole alkaloids from the roots of *Isatis indigotica*. *J Asian Nat Prod Res* 2015;**17**:689−704.
45. Liu YF, Chen MH, Lin S, Li YH, Zhang D, Jiang JD, et al. Indole alkaloid glucosides from the roots of *Isatis indigotica*. *J Asian Nat Prod Res* 2016;**18**:1−12.
46. Liu Y, Wang X, Chen M, Lin S, Li L, Shi J. Three pairs of alkaloid enantiomers from the root of *Isatis indigotica*. *Acta Pharm Sin B* 2016;**6**:141−7.
47. Chen MH, Lin S, Wang YN, Zhu CG, Li YH, Jiang JD, et al. Antiviral stereoisomers of 3,5-bis(2-hydroxybut-3-*en*-1-yl)-1,2,4-thiadiazole from the roots of *Isatis indigotica*. *Chin Chem Lett* 2016;**27**:643−8.
48. Liu Y, Chen M, Guo Q, Li Y, Jiang J, Shi J. Aromatic compounds from an aqueous extract of "ban lan gen" and their antiviral activities. *Acta Pharm Sin B* 2017;**7**:179−84.
49. Meng L, Guo Q, Liu Y, Chen M, Li Y, Jiang J, et al. Indole alkaloid sulfonic acids from an aqueous extract of *Isatis indigotica* roots and their antiviral activity. *Acta Pharm Sin B* 2017;**7**:334−41.
50. Meng L, Guo Q, Liu Y, Shi J. 8,4′-Oxyneolignane glucosides from an aqueous extract of "ban lan gen" (*Isatis indigotica* root) and their absolute configurations. *Acta Pharm Sin B* 2017;**7**:638−46.
51. Meng LJ, Guo QL, Xu CB, Zhu CG, Liu YF, Chen MH, et al. Diglycosidic indole alkaloid derivatives from an aqueous extract of *Isatis indigotica* roots. *J Asian Nat Prod Res* 2017;**19**:529−40.
52. Guo Q, Xu C, Chen M, Lin S, Li Y, Zhu C, et al. Sulfur-enriched alkaloids from the root of *Isatis indigotica*. *Acta Pharm Sin B* 2018;**8**:933−43.
53. Meng LJ, Guo QL, Zhu CG, Xu CB, Shi JG. Isatindigodiphindoside, an alkaloid glycoside with a new diphenylpropylindole skeleton from the root of *Isatis indigotica*. *Chin Chem Lett* 2018;**29**:119−22.
54. Meng L, Guo Q, Chen M, Jiang J, Li Y, Shi J. Isatindolignanoside A, a glucosidic indole-lignan conjugate from an aqueous extract of the *Isatis indigotica* roots. *Chin Chem Lett* 2018;**29**:1257−60.
55. Hu M, Xu C, Yang C, Zuo H, Chen C, Zhang D, et al. Discovery and evaluation of ZT55, a novel highly-selective tyrosine kinase inhibitor of $JAK2^{V617F}$ against myeloproliferative neoplasms. *J Exp Clin Cancer Res* 2019;**38**:49.
56. Li DW, Guo QL, Meng XH, Zhu CG, Xu CB, Shi JG. Two pairs of unusual scalemic enantiomers from *Isatis indigotica* leaves. *Chin Chem Lett* 2016;**27**:1745−50.
57. Nakanishi K, Berova N, Woody N. *Circular dichroism: principles and applications*. New York: Wiley-VCH; 1994. p. 413−72.
58. Li XC, Ferreira D, Ding Y. Determination of absolute configuration of natural products: theoretical calculation of electronic circular dichroism as a tool. *Curr Org Chem* 2010;**14**:1678−97.
59. Xu LH, Huang F, Cheng T, Wu J. Antivirus constituents of radix of *Isatis indigotica*. *Chin J Nat Med* 2005;**3**:359−60.